

Levels in Ni^{57} from the $\text{Ni}^{58}(\text{He}^3, \alpha)\text{Ni}^{57}$ Reaction*

CHENG-MING FOU AND ROBERT W. ZURMÜHLE

Department of Physics, University of Pennsylvania, Philadelphia, Pennsylvania

(Received 2 July 1965)

Levels in Ni^{57} were studied by detecting the α particles from the $\text{Ni}^{58}(\text{He}^3, \alpha)\text{Ni}^{57}$ reaction in a 24-in. diam scattering chamber using surface-barrier solid-state detectors. The Q value of the reaction was measured to be 8.40 ± 0.05 MeV. Excited levels in Ni^{57} at 0.75, 1.05, 2.55, 3.25, 3.70, 3.85, 4.25, 4.55, 4.95, 5.25, 5.57, 5.85, 6.05, 6.97, 7.15, 7.85 MeV were observed. Angular distributions of elastically scattered He^3 , as well as those of α particles leading to ground, 0.75-, 1.05-, 2.55-, 3.25-, 5.25-, 5.57-, and 6.05-MeV states have been measured. γ rays, in coincidence with the reaction α particles, have also been observed with a 3 in. \times 4 in. NaI(Tl) crystal and analyzed with a 2-parameter pulse-height analyzer to study the decay scheme of the excited states. Distorted-wave analysis, using the Oak Ridge National Laboratory's JULIE computer code, yielded the following spin assignments: ground state, $l=1$; 0.75-MeV state, $l=3$; 1.05-MeV state, $l=1$; 2.55-, 3.25-, 5.25-, 5.57-MeV states, all $l=3$; 6.05-MeV state, either $l=2$ or $l=3$. Relative spectroscopic factors of these states have been extracted.

INTRODUCTION

THE structure of Ni^{57} is of interest because in its ground state it can be considered as consisting of a double closed $f_{7/2}$ core plus one neutron. Previous studies have been made with $\text{Ni}^{58}(d, t)\text{Ni}^{57}$ and the $\text{Ni}^{58}(p, d)\text{Ni}^{57}$ reactions.^{1,2} However, because of the large negative Q values of these two reactions, only states up to 2.6-MeV excitation have been reported. The present experiment utilizes the high positive Q value of the (He^3, α) reaction to study higher excited states in Ni^{57} . At the same time distorted-wave Born approximation (DWBA) analysis is applied to gain spectroscopic information about the observed states.

EXPERIMENTAL DETAILS

The reaction was studied in a 24-in. scattering chamber with a 15- and 18-MeV He^3 beam from the University of Pennsylvania tandem accelerator. The design and the operation of the scattering chamber have been described elsewhere.³ The 99.9% enriched self-supporting Ni^{58} target was provided by Stable Isotope Division of Oak Ridge National Laboratory and was about $500 \mu\text{g}/\text{cm}^2$ thick. 500- μ -thick surface-barrier solid-state detectors of 50 mm^2 sensitive area were used for the particle detection. The maximum energy loss of protons in such detectors is about 9 MeV. Therefore, angular distributions of α particles with energies higher

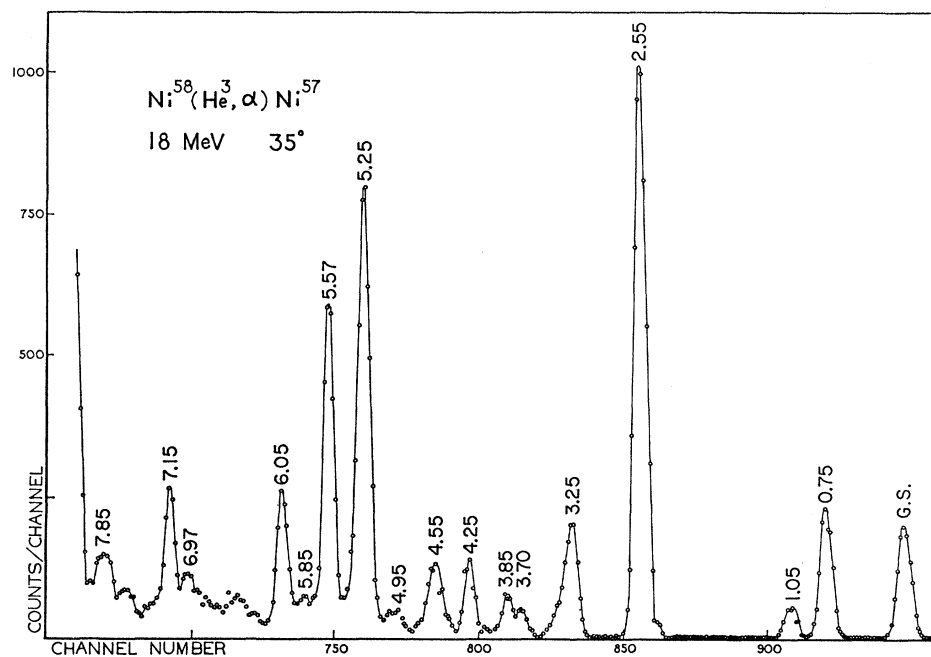


FIG. 1. Spectrum of α particles obtained from $\text{Ni}^{58}(\text{He}^3, \alpha)\text{Ni}^{57}$ reaction at 35° , incident He^3 beam energy 18 MeV (G. S. \equiv ground state).

* Supported by the National Science Foundation.

¹ M. H. Macfarlane, B. J. Raz, J. L. Yntema, and B. Zeidman, Phys. Rev. **127**, 204 (1962).

² J. C. Legg and E. Rost, Phys. Rev. **134**, B752 (1964).

³ R. W. Zurmühle, Nucl. Instr. Methods **36**, 168 (1965).

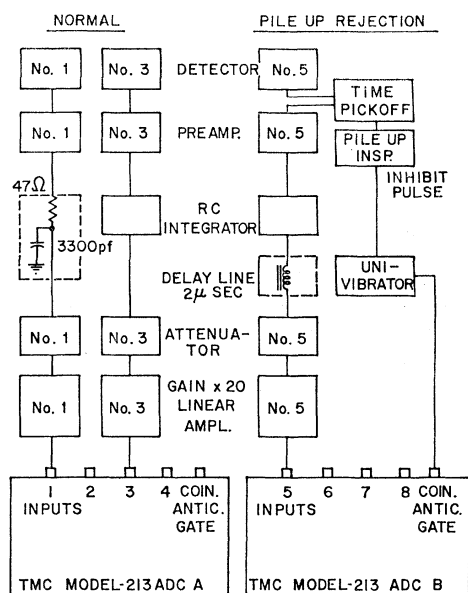


FIG. 2. Electronics block diagrams for angular distribution measurements.

than the elastically scattered He^3 can be measured without particle identification. Angular distributions of elastically scattered He^3 were also obtained. Eight movable detectors were used simultaneously with a monitoring detector which was placed at 45° . The detectors were placed 10° apart and $6\frac{1}{2}$ in. from the target. Angular distributions were measured in 5° intervals from 10° to 175° . Pile-up rejection was applied for the measurement at 10° and 15° using the ORTEC Model 240+242 time pickoff and pile-up inspector system. This reduced the background due to the pile-up of pulses from elastically scattered He^3 . A typical α -particle spectrum is shown in Fig. 1.

The decay scheme of the excited states was studied by observing γ rays in coincidence with the α particles. The particle detector was placed at 35° to the right of the beam, $1\frac{1}{2}$ in. from the target. The γ detector was a 3-in. \times 4-in. NaI(Tl) crystal placed at 45° to the left of the beam with the front surface 3 in. from the target. The pulses from both detectors were fed into a TMC-4096

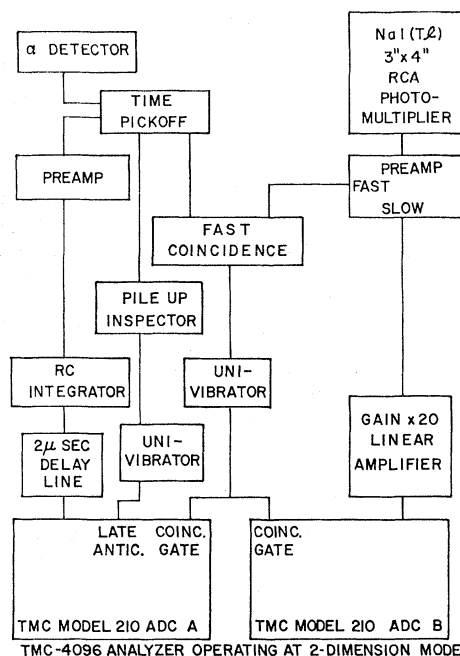


FIG. 3. Electronics block diagrams for decay-scheme study by α - γ coincidence measurements.

two-parameter analyzer which was gated by the output of a fast coincidence circuit. The time resolution of the coincidence circuit was adjusted to about 60 nsec. Electronics block diagrams are shown in Figs. 2 and 3.

The absolute cross sections of the reaction are calculated by comparison with the elastic He^3 scattering cross section, assuming that the scattering is purely Rutherford scattering at angles less than 20° . The uncertainty of these cross sections is approximately 30%.

EXPERIMENTAL RESULTS

The measured Q value of this reaction is 8.40 ± 0.05 MeV. This is consistent with the Q value obtained from the $\text{Ni}^{58}(p,d)\text{Ni}^{57}$ reaction,² both Q values lying about 250 keV below the values given in Nuclear Data Tables. Sixteen excited levels in Ni^{57} are identified (see Fig. 4). The uncertainties of the excitation energies are about ± 50 keV. Angular distributions of eight well resolved

TABLE I. Searched optical-potential parameters of the entrance channel, obtained by analyzing the elastic-scattering data of He^3 by Ni^{58} at 15 and 18 MeV using the HUNTER computer code.

Name	Incident energy (MeV)	V (MeV)	W (MeV)	r_v (F)	r_w (F)	a_v (F)	a_w (F)	r_c (F)
(i) He^3 -30	15	34.3	12.9	1.67	1.67	0.58	0.58	1.40
	18	31.3	16.1	1.67	1.67	0.58	0.58	1.40
(ii) He^3 -100	15	107.5	15.1	1.07	1.70	0.854	0.754	1.40
	18	106.1	19.2	1.07	1.70	0.854	0.754	1.40
(iii) He^3 -180	15	180.0	30.0	0.73	1.56	0.960	0.864	1.40
	18	180.0	35.0	1.06	1.50	0.733	0.835	1.40

TABLE II. Optical-potential parameter sets for the exit channel used in the distorted-wave calculations using the JULIE computer code.

Name	Incident energy (MeV)	V (MeV)	W (MeV)	r _v (F)	r _w (F)	a _v (F)	a _w (F)	r _e (F)
(1) α-47	28	47.6	13.8	1.585	1.585	0.549	0.549	1.40
(2) α-67	21	67.4	12.8	1.586	1.586	0.522	0.409	1.40
(3) α-79	24	79.0	12.0	1.52	1.52	0.60	0.60	1.40
(4) α-134	21	134.3	10.9	1.466	1.466	0.517	0.517	1.40

states are obtained. Strong γ transitions which could be identified from the spectra observed in the α-γ coincidence measurement are shown in Fig. 5. From the 5.57-MeV state the transition to the ground state is rather weak, and the transition to the 4.55-MeV state is given here only tentatively. This is because the decay schemes of the levels between 5.25- and 3.25-MeV states, which are excited only weakly by the present reaction, are not well known. Thus, the identification is rather difficult. No other distinct transitions from the 5.57-MeV states are observed. The transitions from the 5.25- to the 2.55-MeV state, for the same reason mentioned above, are given only tentatively.

THE DWBA ANALYSIS

The Oak Ridge National Laboratory automatic-search computer code, HUNTER,⁴ is used to analyze the

He³ elastic scattering data for determining the optical potential parameters of the entrance channel. The Saxon-Woods-type potential used is

$$V(r) = -\frac{V}{\exp[(r-r_v A^{1/3})/a_v]+1} - \frac{iW}{\exp[(r-r_w A^{1/3})/a_w]+1}$$

Three sets of parameters are obtained, as shown in Table I. The searches which lead to these parameter sets are biased in the following ways:

- (i) The geometrical parameters are kept equal to those obtained by Blair and Wegner⁵ from the analysis of He³ elastic scattering by Fe⁵⁶.

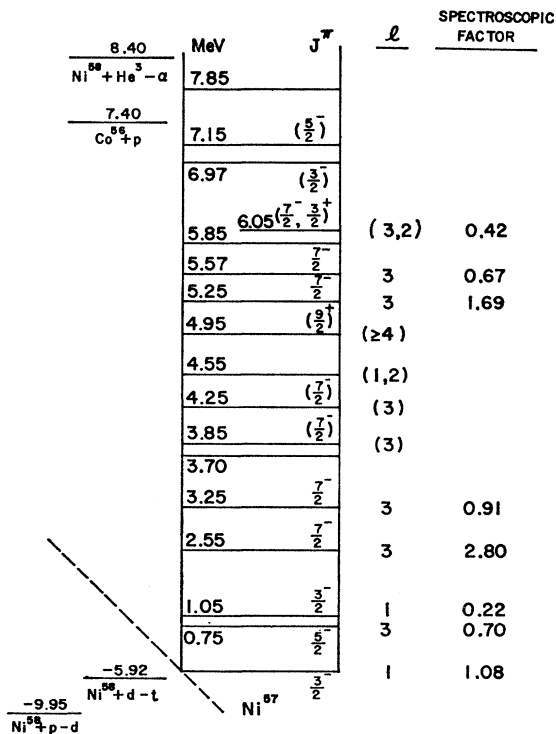


FIG. 4. Energy-level structure of Ni⁵⁷.

⁴ R. M. Drisko (unpublished).

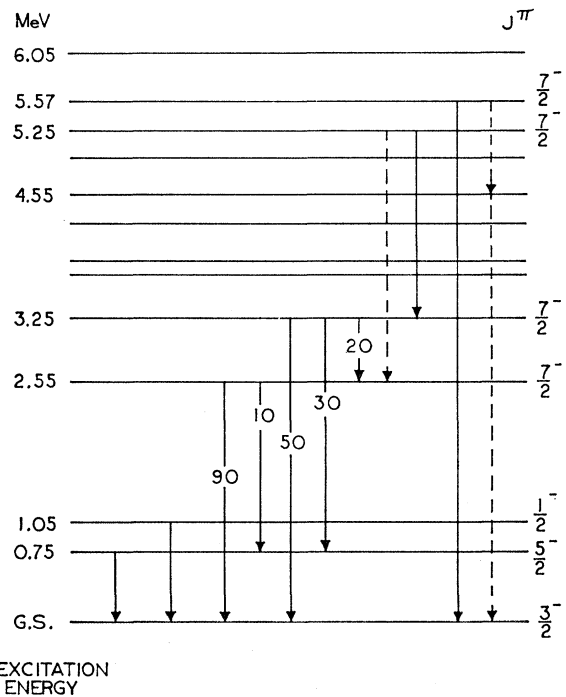


FIG. 5. Decay scheme of excited states in Ni⁵⁷ based on the α-γ coincidence measurement with gamma detector at 45° to the left and alpha detector at 35° to the right of the beam. Uncertainties of the relative intensities shown are ±10%.

⁵ A. G. Blair and H. E. Wegner, Phys. Rev. 127, 1233 (1962).

(ii) The geometrical parameters are kept equal to those obtained by Bassel⁶ from the analysis of He³ elastic scattering by various nuclei ranging from Mg²⁴ to Zr⁹⁰.

(iii) The real-well depth is kept to be 180 MeV deep.

For the exit channel, again, a Saxon-Woods type potential is used. Optical-potential parameters, obtained from analyzing α -particle elastic scattering by Ni⁵⁸ and Fe⁵⁶ are adopted.^{5,7} These parameters are shown in Table II. All combinations of the entrance- and the exit-channel parameter sets are used to calculate the theoretical angular distributions of the ground and 2.55-MeV states for both 15 and 18 MeV. All combinations give fairly good shape fits by assuming $l=1$ for the ground state and $l=3$ for the 2.55-MeV state. However, the maxima and minima are shifted by 5° to 10° with respect to the experimental angular distribution. The only complete fits to the experimental angular distributions for both 15 and 18 MeV are obtained with the combination of entrance-channel parameter set (i) with exit-channel parameter set (3). This combination is, therefore, used for the spin assignments of other states. Because of the difference of the α particles' energies leading to the different excited states in Ni⁵⁷ and the fact that the parameter set (3) is obtained from 24-MeV α -particle elastic scattering data, the real potential-well depths of the exit channel have to be adjusted accordingly.⁸ This is done in the following way: The real-well depth 79 MeV is increased or decreased by the same amount that the α -particle energy differs from 24-MeV—deeper well for α particles with lower energies and vice versa. The predicted angular distributions are not strongly affected by this procedure; yet the adjustments do supply slightly better fits, as shown in Figs. 6 and 7. The l values obtained are listed in Fig. 4. The 0.75-MeV state has been observed in the (p,d) reaction. Its angular distribution showed an $l=1$ contribution. Since the present (He³, α) reaction, due to its large positive Q value, favors the excitation of high angular-momentum states, our angular distribution does not reveal the $l=1$ contribution, but it also does not exclude this possibility. The (p,d) result seems to suggest that there are two unresolved states at 0.75 MeV.

⁶ J. L. Yntema, B. Zeidman, and R. H. Bassel, Phys. Letters **11**, 302 (1964).

⁷ R. H. Bassel (private communication).

⁸ The dependence of the optical potential-well depths for protons and neutrons on their incident energies has been empirically established. See, for example, Hodgson, *The Optical Model of Elastic Scattering* (The Clarendon Press, Oxford, 1963). The real-well depth decreases with increasing incident energy while the imaginary-well depth increases slowly with increasing incident energy. This is generally understood to be the result of averaging over the nucleon-nucleon potentials and of the Pauli principle, and should apply just as well to composite incident particles. However, because of insufficient data, no empirical formula has been established so far. The searched He³ parameters for 15- and 18-MeV incident energies presented here indicate this trend nicely. The procedure taken here is a guess. The adjustments do provide better fits without affecting the l -value assignment. The extracted spectroscopic factors are affected by less than 5%. Similar adjustment has been applied in other cases, for example, in Ref. 5.

With the knowledge obtained from the distorted-wave fits to the strong and resolved states, some tentative l -value assignments for the weak states can be given. The 4.55-MeV group has a similar angular distribution as that of the ground state, therefore, it could be a $l=1$ or $l=2$ state. The 3.85- and the 4.25-MeV states have characteristic $l=3$ angular distributions. The angular distributions of the 6.97- and 7.15 MeV states are consistent with the assignments $l=1$ and $l=3$, respectively suggested by their analogue states in Co⁵⁷ to be discussed later.

For the 6.05-MeV state, the predicted angular distributions for $l=3$ and $l=2$ are very similar. The 18-MeV experimental angular distribution favors $l=2$ assignment but the 15-MeV one favors $l=3$ assignment.

SPECTROSCOPIC FACTORS

The relative spectroscopic factors extracted from the (He³, α) reaction depend strongly on the wave function of the transferred neutron. However, the predicted angular distribution is rather insensitive to it. In the present analysis, using the Oak Ridge National Laboratory JULIE⁹ code, the neutron wave function is calculated from a real Saxon-Woods type potential with the well depth determined by the given shell-model orbitals and binding energy. Different ways of determining the binding energy are tried and the relative spectroscopic factors extracted are shown in Table III. In group (I) all the wave functions are calculated from the same well. In group (II) the binding energies are equal to the separation energies. In group (III) the binding energies of all states with $l=3$ except the 0.75-MeV state are equal to the separation energy of the neutron leaving the residual nucleus Ni⁵⁷ in the 5.25-MeV state. The choice in group (III) is made based on the assumption that all of these $l=3$ states result from the splitting of one 7/2⁻ hole state and that their center is somewhere around the 5.25-MeV state. The 0.75-MeV state is excluded because it is believed to be a 5/2⁻ state. Arguments are given in the next paragraph. The well depths for the transferred neutron in each case are shown in Table IV.

NORMALIZATION OF THE SPECTROSCOPIC FACTORS

The 0.75-MeV state has been assigned to be $l=3$. It was suggested by Macfarlane *et al.*¹ to be 5/2⁻, resulting from pickup of one neutron out of the ($f_{5/2}$)²₀ configuration which is mixed into the ground state of Ni⁵⁸. If we further assume that the 1.05-MeV state is also resulting from pickup of one of the two neutrons outside the double closed $f_{7/2}$ core in Ni⁵⁸, then we can normalize the sum of the relative spectroscopic factors of the ground, 0.75-, 1.05-MeV states to 2. The spectroscopic factor of the 1.05-MeV state then becomes 0.22. The occupation

⁹ R. H. Bassel, R. M. Drisko, and G. R. Satchler (unpublished).

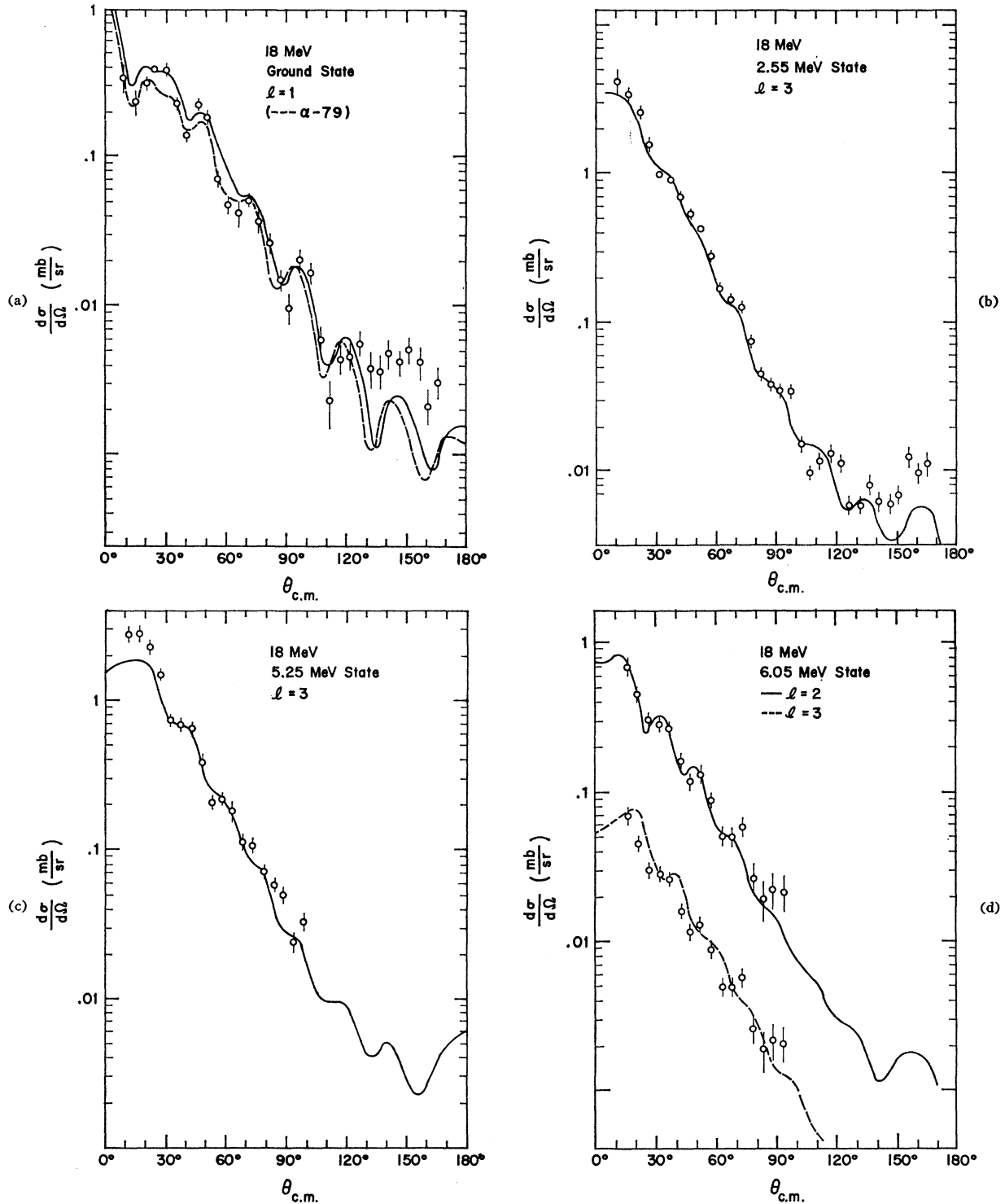


FIG. 6. (a) Angular distribution of α particles from the $\text{Ni}^{58}(\text{He}^3, \alpha)\text{Ni}^{57}$ reaction leading to the ground state in Ni^{57} . The laboratory energy of the He^3 beam was 18.110 ± 0.020 MeV. The solid line results from DWBA calculations normalized to the data. The parameters used are: for the entrance channel, (i) and for the exit channel, (3) (with V adjusted to 76 MeV to take into account the high α -particle energy) listed in Tables II and III, respectively. (b) Angular distribution for the 2.55-MeV state. Condition same as for Fig. 6(a), except the V in exit channel parameter set (3) is 79 MeV. (c) Angular distribution for the 5.25-MeV state. Condition same as for Fig. 6(a), except the V in exit channel parameter set (3) is adjusted to 81 MeV to take into account the low α -particle energy. No data points are available beyond 100° because the measurement was taken by reflection, so this state is no longer well resolved. (d) Angular distribution for the 6.05-MeV state. Condition same as for Fig. 6(a), with $V=81$ MeV in the exit channel. No data points are available beyond 100° for the same reason given for Fig. 6(c). Solid line assuming $l=2$, dashed line $l=3$.

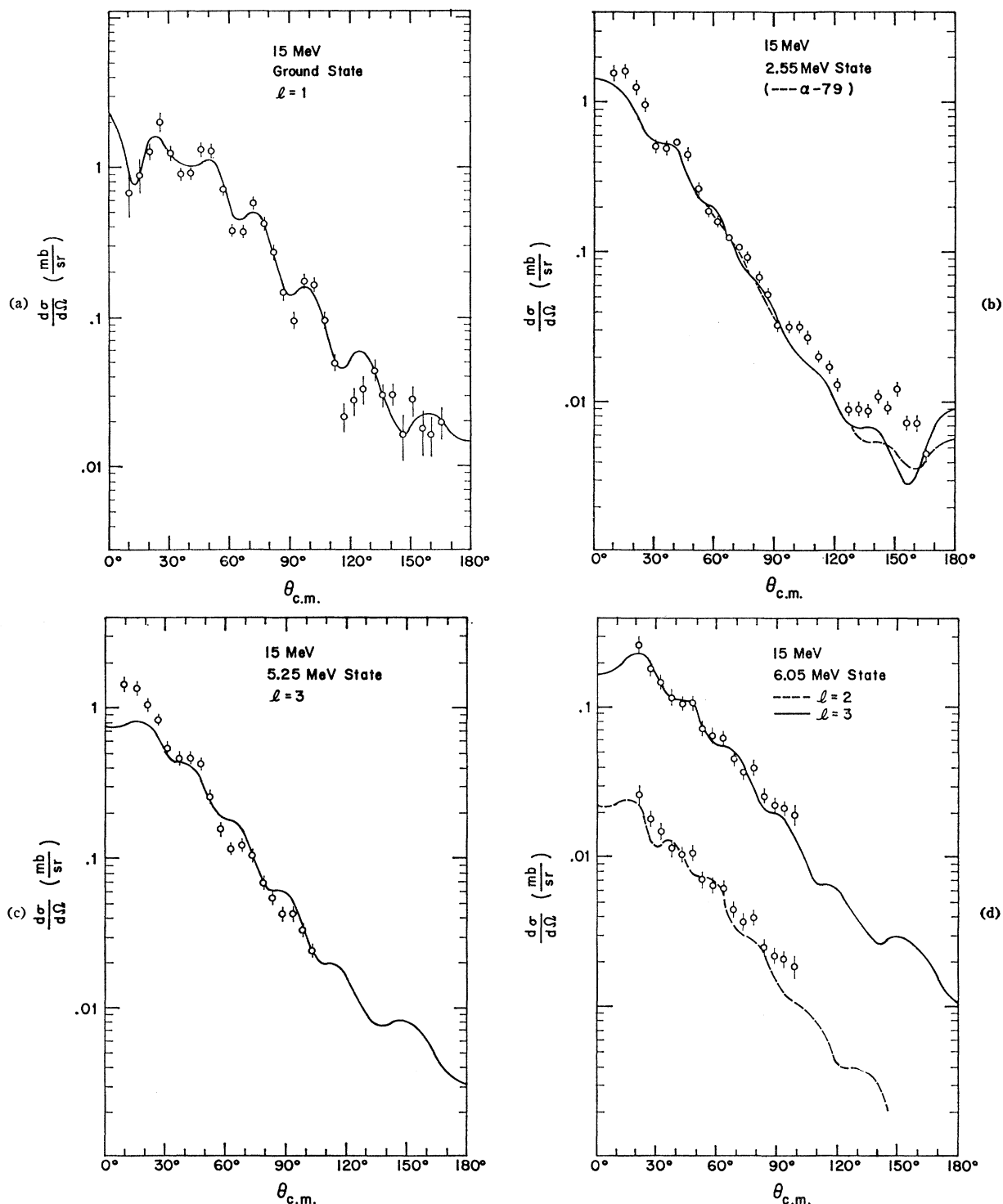


FIG. 7. (a) Angular distribution of α particles from $\text{Ni}^{58}(\text{He}^3, \alpha)\text{Ni}^{57}$ leading to the ground state in Ni^{57} . The laboratory energy of the He^3 beam was 15 MeV. The solid line results from distorted-wave calculations normalized to the data. The parameters used are: for the entrance channel, (1) and for the exit channel, (3) listed in Tables II and III, respectively. (b) Angular distribution for the 2.55-MeV state. Condition same as for Fig. 7(a), except V is adjusted to 82 MeV in the exit channel to take into account the low α energy. Dashed line results from keeping $V=79$ MeV. (c) Angular distribution for the 5.25-MeV state. Condition same as for Fig. 7(a), except V is adjusted to 84 MeV. No data are available beyond 100° because the measurements were taken by reflection, so that the state was no longer well resolved. (d) Angular distribution for the 6.05-MeV state. Condition same as for Fig. 7(a), except V is adjusted to 84 MeV. No data points beyond 100° for the same reason as for Fig. 7(c). Dashed line results from assuming $l=2$.

TABLE III. Relative spectroscopic factors extracted from comparison of experimental data with the distorted-wave calculations using different neutron wave functions.

Group (I). All neutron wave functions calculated with the Saxon-Woods real potential well $V(r) = -V/(e^x + 1)$, $x = (r - r_0 A^{1/3})/a$, with $V = 59.6$ MeV, $r_0 = 1.2$ F, $a = 0.65$ F. This well depth is determined by requiring that the binding energy of a $2p$ neutron be equal to the separation energy of a neutron which leaves the residual nucleus Ni⁵⁷ in its ground state.

Group (II). All neutron wave functions calculated with the assumption, binding energy equal to separation energy. The resulting well depths are shown in Table IV.

Group (III). All $1f_{7/2}$ neutron wave functions are calculated with binding energies equal to the separation energy of the neutron which leaves the residual nucleus Ni⁵⁷ in the 5.25-MeV state. Consequently, their well depths are all equal to 63.3 MeV, as given in Table IV. The sum of the spectroscopic factors of the ground state, the 0.75-, and the 1.05-MeV states is normalized to 2, because they are the states resulting from picking up one of the two neutrons in Ni⁵⁸ which are outside of the double closed $f_{7/2}$ core. The sums of the spectroscopic factors of the $7/2^-$ states in Groups (II) and (III) exceed 8—the total number of $f_{7/2}$ neutrons in Ni⁵⁸. It seems to indicate that the procedures of calculating the neutron wave functions used in (II) and (III) are not correct. N are normalization factors; the theoretical value is calculated from the He³ and α -particle wave-function overlap using zero-range approximation. The experimental values for N for 18- and 15-MeV data are determined from normalizing the sum of the spectroscopic factors of the first three states to 2.

State	Spin parity	$\sigma_{\text{expt}} = NS\sigma_{\text{theor}}$ $N_{(18 \text{ MeV})} = 47$		$N_{(15 \text{ MeV})} = 31$		$N_{(18 \text{ MeV})} = 1.63$ $N_{(15 \text{ MeV})} = 31$	
		(I) 18 MeV	(I) 15 MeV	(II) 18 MeV	(II) 15 MeV	(III) 18 MeV	(III) 15 MeV
Ground	3/2 ⁻	1.10	1.06	1.10	1.06	1.10	1.06
0.75 MeV	5/2 ⁻	0.69	0.71	0.69	0.71	0.69	0.71
1.05 MeV	1/2 ⁻	0.21	0.23	0.21	0.23	0.21	0.23
		2.00	2.00	2.00	2.00	2.00	2.00
2.55 MeV	7/2 ⁻	2.88	2.71	2.88	2.71	5.15	4.97
3.25 MeV	7/2 ⁻	0.81	1.01	0.81	1.01	1.26	1.59
5.25 MeV	7/2 ⁻	1.66	1.72	3.12	3.22	3.11	3.21
5.57 MeV	7/2 ⁻	0.70	0.63	1.38	1.27	1.32	1.19
6.05 MeV	7/2 ⁻	0.45	0.38	1.00	0.85	0.82	0.72
		6.50	6.45	9.19	9.06	11.66	11.68

numbers of the configurations in the ground state of Ni⁵⁸ as calculated by Kisslinger and Sorensen¹⁰ are

$$(p_{3/2})^2_0 : (f_{5/2})^2_0 : (p_{1/2})^2_0 = 1.28 : 0.58 : 0.08.$$

The levels in Ni⁵⁷ assumed by them in their calculation are

$$\begin{aligned} p_{3/2}, & 0.00 \text{ MeV}; \\ f_{5/2}, & 0.78 \text{ MeV}; \\ p_{1/2}, & 1.56 \text{ MeV}. \end{aligned}$$

Comparing these results with our spectroscopic factors, they suggest that the 1.05-MeV state is a $1/2^-$ state resulting from pickup of one neutron out of the $(p_{1/2})^2_0$ configuration mixed into the ground state of Ni⁵⁸.

Using this normalization, the sums of the rest of the $l=3$ states in different groups in Table III turn out to be 6.5, 9.1, 11.7, respectively. The DWBA predicted cross section turns out to be smaller than the measured cross section by a factor of 29 in the 18-MeV case and by a factor of 20 in the 15-MeV case. Similar discrepancies have been observed in the DWBA analysis^{11,12} of O¹⁶(He³, α)O¹⁵ and Ca⁴⁰(He³, α)Ca³⁹ reactions. This disagreement between theory and experiment is believed to be at least partly due to the zero-range approximation and the local potential used in the calculation.

¹⁰ L. S. Kisslinger and R. A. Sorensen, Kgl. Danske Videnskab. Selskab, Mat. Fys. Medd. 32, No. 9 (1960).

¹¹ W. P. Alford, L. M. Blau, and D. Cline, Nucl. Phys. 61, 368 (1965).

¹² D. Cline, L. M. Blau, and W. P. Alford, Nucl. Phys. (to be published).

Co⁵⁷ ANALOG STATES

The Coulomb energy difference between Ni⁵⁷ and Co⁵⁷ can be calculated using the semiclassical formula assuming uniform charge distribution.¹³ If we use the radius $r_0 A^{1/3}$ with $r_0 = 1.27$ F determined by high-energy electron-scattering measurements assuming uniform charge distribution, we get

$$\Delta E_{\text{Coul}} = 9.24 \text{ MeV}.$$

Subtracting the neutron proton mass difference of 1.29 MeV and the Ni⁵⁷-Co⁵⁷ nuclei mass difference of

TABLE IV. Potential well for the transferred neutron. The neutron well depths are obtained by requiring the binding energies to be equal to the separation energies.

State in residual nucleus (MeV)	Shell-model orbital of the neutron	Binding energy (MeV)	Well depth V (MeV)
Ground	$2p$	12.18	59.5
0.75	$1f$	12.93	57.1
1.05	$2p$	13.23	61.1
2.55	$1f$	14.73	59.6
3.25	$1f$	15.43	60.6
5.25	$1f$	17.43	63.3
5.57	$1f$	17.75	63.8
6.05	$1f$	18.23	64.4
	$1d$	18.23	48.7

¹³ S. Sengupta, Nucl. Phys. 21, 542 (1960).

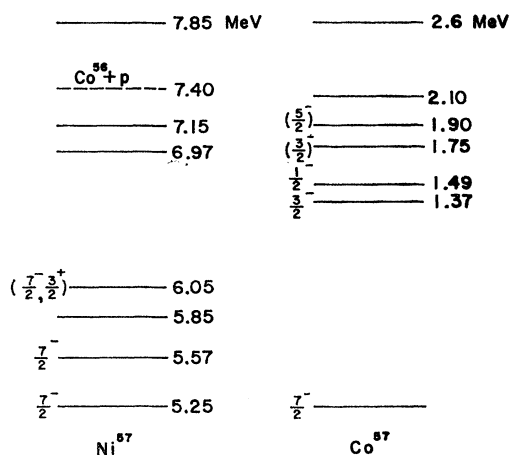


FIG. 8. Comparison of Co^{57} levels with Ni^{57} levels in the analog states region.

2.75 MeV, the excitation of the lowest $T=3/2$ state in Ni^{57} turns out to be 5.2 MeV. The 5.25-MeV state in Ni^{57} is, therefore, most likely the analog state of the Co^{57} ground state. Our spin assignment, $7/2^-$, is also consistent with this assumption. The 2.55-MeV state ($7/2^-$) consequently could be the conjugate ($T=1/2$, $T_z=1/2$) state.

A comparison of the low-lying states^{14,15} in Co^{57} with the higher excited states in Ni^{57} is shown in Fig. 8. Looking at the spectrum of Ni^{57} , shown in Fig. 1, at excitation energies where one expects to see the analog states of the 1.37- and 1.49-MeV states in Co^{57} , no strong states can be seen. The weak excitation of these states in Ni^{57} allows some conclusions regarding their configurations to be made. It could, for example, be explained if the 1.37- and 1.49-MeV states in Co^{57} were states with two proton holes in the $f_{7/2}$ shell and one proton in the $p_{3/2}$ or $p_{1/2}$ state. Their analog states in Ni^{57} would not be excited strongly by the $\text{Ni}^{58}(\text{He}^3, \alpha)\text{Ni}^{57}$ reaction, since this reaction creates only one neutron hole in the $f_{7/2}$ shell. However, the 6.97- and the 7.15-MeV states in Ni^{57} line up with the 1.75- and 1.90-MeV states in

Co^{57} , and the 7.85-MeV state in Ni^{57} lines up with the 2.6-MeV state¹⁶ in Co^{57} .

SUMMARY

The spectroscopic information about the configuration of the ground state of Ni^{58} obtained from the experimental data of the low-lying states in Ni^{57} is in agreement with the calculation of Kisslinger and Sorensen.⁹ The $f_{7/2}$ hole state is strongly excited and is split into several levels.

The DWBA analysis of the (He^3, α) reaction gives very good fits to the angular distribution for l -value assignments. However, the predicted cross-section is too small by a factor of roughly 20 to 29. Similar factors have been obtained from the DWBA analysis of (He^3, α) reaction on O^{16} and Ca^{40} . Furthermore, only a certain combination of the optical potential parameter sets of the entrance and exit channels produces good fits to the measured reaction angular distribution in the DWBA analysis. It would be interesting to investigate the physical reason for this and thus reduce some ambiguity of the parameter sets.

The study of the decay schemes of the $7/2^-$ states in Ni^{57} presents an interesting example of investigation of configurations. More reliable information can be obtained if theoretical calculations are performed to predict the transition probabilities between the various configurations.

ACKNOWLEDGMENTS

We are indebted to R. H. Bassel for his advice in the DWBA analysis and to A. Klein for several clarifying discussions. The helpful suggestions and assistance of the whole tandem accelerator group, especially that of W. E. Stephens, R. Middleton, C. Holbrow, and J. M. Joyce, are appreciated.

We would also like to thank the Oak Ridge National Laboratory for the use of its computer facilities.

¹⁴ S. E. Arnell and P. O. Persson, *Arkiv Fysik* **26**, 193 (1964).

¹⁵ B. L. Cohen, *Phys. Rev.* **108**, 768 (1957).

¹⁶ This state has, so far, been seen in the $\text{Ni}^{58}(p, 2p)\text{Co}^{57}$ reaction (Ref. 15) only, although the 2.64-MeV gamma line reported in Ref. 14, but not fitted in their decay scheme, might be from the same state.